Tribol Lett (2010) 38:135–146
DOI 10.1007/s11249-010-9582-8

ORIGINAL PAPER

Friction and Wear Behaviour of Brake Pads Dry Sliding Against Semi-Interpenetrating Network Ceramics/Al-alloy Composites

Shao Yang Zhang · Yuan Yuan Li · Sheng Guan Qu · Wei Ping Chen

Received: 30 October 2008 / Accepted: 31 January 2010 / Published online: 12 March 2010

Abstract Semi-interpenetrating network composites containing 40 vol.% ceramics ($5Al_2O_3{\cdot}8SiO_2$) and 60 vol.% Al-alloy were fabricated in place of cast iron available for automotive brake rotors. The friction and wear performances of brake pads dry sliding against the composites were measured using a SRV testing machine. The test procedures include friction fade and recovery, load sensitivity at 100 and 250°C, and wear. The friction was found to increase first and then decrease with increasing temperature, followed by the inverse recovery upon cooling. Wear showed an incremental tendency over a wide temperature range. For loads from 40 to 160 N, the friction decreased at 100 and 250°C. At load below 128 N, the former friction was inferior to the latter while at load above 128 N the friction exhibited an inverse tendency. Wear mildly increased with load at 100 °C and decreased dramatically at 250 °C. SEM and EDS investigations revealed that the worn pad surfaces at 250 °C were covered by more tribofilms, including more coke and graphite with friction-reducing action as well as fewer compounds (corresponding to Si and Al) with friction-increasing action in comparison with those at 100 °C. The compression of the tribofilms contributed to a large decrease in the friction and wear with increasing load. However, at 100 °C E-glass fibers exposed at the worn surfaces inhibited the excessive wear of the pad despite lack of more tribofilms. Their glossy surfaces decreased the friction. The proposed friction models explain some friction and wear behaviour better.

Keywords Brake pad · Semi-interpenetrating network composites · Friction · Wear

1 Introduction

Al-alloy is widely attractive for the aerospace, automobile, electron and electric fields with good features of low density, high thermal conductivity and easy-machining [1, 2]. Nevertheless, it is unable to be applied solely to automotive brake rotors in spite of its light weight. This necessitates higher hardness, wear-resistant materials with the combination of it to remedy its performance deficiencies. Taking into account the fact that high hardness materials such as SiC and Al_2O_3 are easy to do damage to brake pads, mullite crystals ($3Al_2O_3{\cdot}2SiO_2$) or the corresponding ceramics is relatively ideal for the friction applications since pure mullite have moderate hardness. Seen from a materials viewpoint, the development trend of advanced new-style automotive brake rotors is to achieve light-weight, high mechanical properties, steady-state friction level and moderate wear. Lightweight components mean greater payload and the additional costs are readily justified. Many experimental studies have been conducted on the ceramic particle-reinforced aluminum metal matrix composites (Al-MMCs) to obtain light-weight brake rotors over the past several decades [3]. A crucial issue concerning poor wetness between the ceramic particles and Al-alloy was raised although various Al-MMCs have successfully been fabricated. One of the interesting results of this work is the difficulty in attempting to employ large

S. Y. Zhang · Y. Y. Li (✉) · S. G. Qu · W. P. Chen
National Engineering Research Center of Near-net-shape Forming for Metallic Materials, School of Mechanical and Automotive Engineering, South China University of Technology, No. 381, Wushan Road, Tianhe District, 510640 Guangzhou, People's Republic of China
e-mail: mehjli@scut.edu.cn

S. Y. Zhang
e-mail: zhshy@scut.edu.cn

amounts of ceramic particles which are blended into molten Al-alloy. In order to lessen the impact of the wetness-dependence and promote the integral structure strength for the composites, a honeycomb-like mullite ceramic preform produced by general methods instead of the ceramic particles was immersed into a molten Al-alloy bath in the present investigation. The Al-alloy was infiltrated into non-interconnected open porosity of the preform under squeezing action through a die in such a manner that a composite toughened by Al-alloy was synthesized when cooled to room temperature. The type of semi-interpenetrating network ceramics/Al-alloy composites can easily hold higher ceramic contents.

In the case of brake pads, the friction level is of primary significance, wear resistance being of secondary one. Considerable attention should be focused on the frictional performance assessment relevant with temperature and load since speed had less influence on friction [4, 5]. In this article, we elaborate on the fabrication of brake pads and semi-interpenetrating network ceramics/Al-alloy composites. A test schedule was developed to determine friction levels and wear. The pad dry sliding against the composites was measured in an area contact mode on a SRV testing machine to make a fair comparison of the influence of different temperatures and loads on friction and wear. SEM was utilized for the worn pad surface characterization and EDS analysis for determining the ingredients and contents of the surface. The friction models were proposed to analyze the results from the tests.

2 Experiment Preparation and Test Method

2.1 Test Materials and Specimens

The honeycomb-like ceramics used as reinforcement frameworks were purchased from Beijing Jingrui Chuangye Superhard Materials Co., Ltd. The average pore diameter was about 1 mm (Fig. 1a). Obviously, its irregular circular shape was formed through ceramic body deformation during the sintering process. EDS (INCA300, Oxford Co.) analysis showed that the ceramics mainly consisted of 26.70 wt% Al, 21.71 wt% Si and 48.72 wt% O, simply denoted as $5Al_2O_3{\cdot}8SiO_2$ (Fig. 1b). Phi-rho-z method was used to correct the influence of the testing specimen substrate. X-Ray powder diffraction analysis revealed that there were merely mullite crystals, but no alumina crystals detected in the ceramics (Fig. 1c). This means that all the alumina has been converted into mullite crystals and the remainder should be dissociative silicon dioxide. The used Al-alloy had the following chemical composition except Al (in wt%): 5.1–6.1 Zn/2.0–3.0 Mg/1.2–2.0 Cu/0.16–0.30 Cr/0.15 Mn/0.50 Fe/0.50 Si. It was placed in a crucible and heated to 50 °C above its liquidus temperature, the ceramic frameworks to 400 °C, and extrusion mould to 300 °C to avoid the Al-alloy excess cooling when mixing. The preheated ceramic frameworks were placed into to the preheated extrusion mould, and then the melted Al-alloy was poured into the ceramic frameworks. Semi-interpenetrating network ceramics/Al-alloy composites were fabricated through squeezing at a pressure of 70 MPa for the duration of 30 s, where the ceramic matrix remains with a crosslinked network structure but Al-alloy has no mutual bonding. Specimens of 5.0 mm × 8.0 mm were cut from the composites and ground to a thickness of approximately 7.0 mm before polishing by the SiC abrasive papers up to 1,000 grits and then a silk cloth under flowing-water conditions. They were estimated to consist of 40 vol.% ceramics and 60 vol.% Al-alloy through calculation. The average density was 2.7 g cm^{-3}. The surfaces before and after tests were photographed using SEM (LEO 1530 VP, Germany) and the photographs are shown in Fig. 2a and b, respectively.

The investigated brake pad materials consisted of 10/30/2/12/6/12/3/13/12 by wt% of copper fiber/E-glass fiber/wood fiber/elastomer modified phenolic resin (containing HEXA)/coke/graphite/chromite/barite/red iron oxide, respectively. E-glass fibers and copper fibers instead of traditional steel wool fibers were used to escape severe damage caused to counter materials [6]. Wood fibers were selected on the basis of their good dispersive capacity to ameliorate the compatibility of E-glass fibers with the binder resin. Their mixing process is similar to our earlier work in Ref. [7]. The brake materials were moulded on a moderate-tonnage press at a pressure of 60 MPa and temperature of 150 °C for 5-min duration. The semi-manufactured goods were cured in a laboratory oven at 180 °C for 8 h. The average density of finished products was 2.34 g cm^{-3}, with 33 HB. Specimens of 16 mm × 18 mm were cut from the products and ground to a thickness of approximately 7.2 mm before polishing by the fine SiC abrasive papers up to 1,000 grits.

2.2 Test Equipment and Procedure

Friction and wear tests were performed on a SRV testing machine (Optimol Instruments Prüftechnik GmbH). Test frequency, stroke, load, temperature and duration can be preset. Friction force is measured continually by a sensor. The friction coefficient is automatically calculated and recorded throughout the test. Also, wear can be measured through a sensor and recorded but the measurement error is relatively large. The current employed method is the weight loss one later in Sect. 2.3. Figure 3 gives a typical oscillation test chamber. A new set of holder was specially designed and fabricated to be suitable for area contact testing in view of the difficulty in machining some ceramic

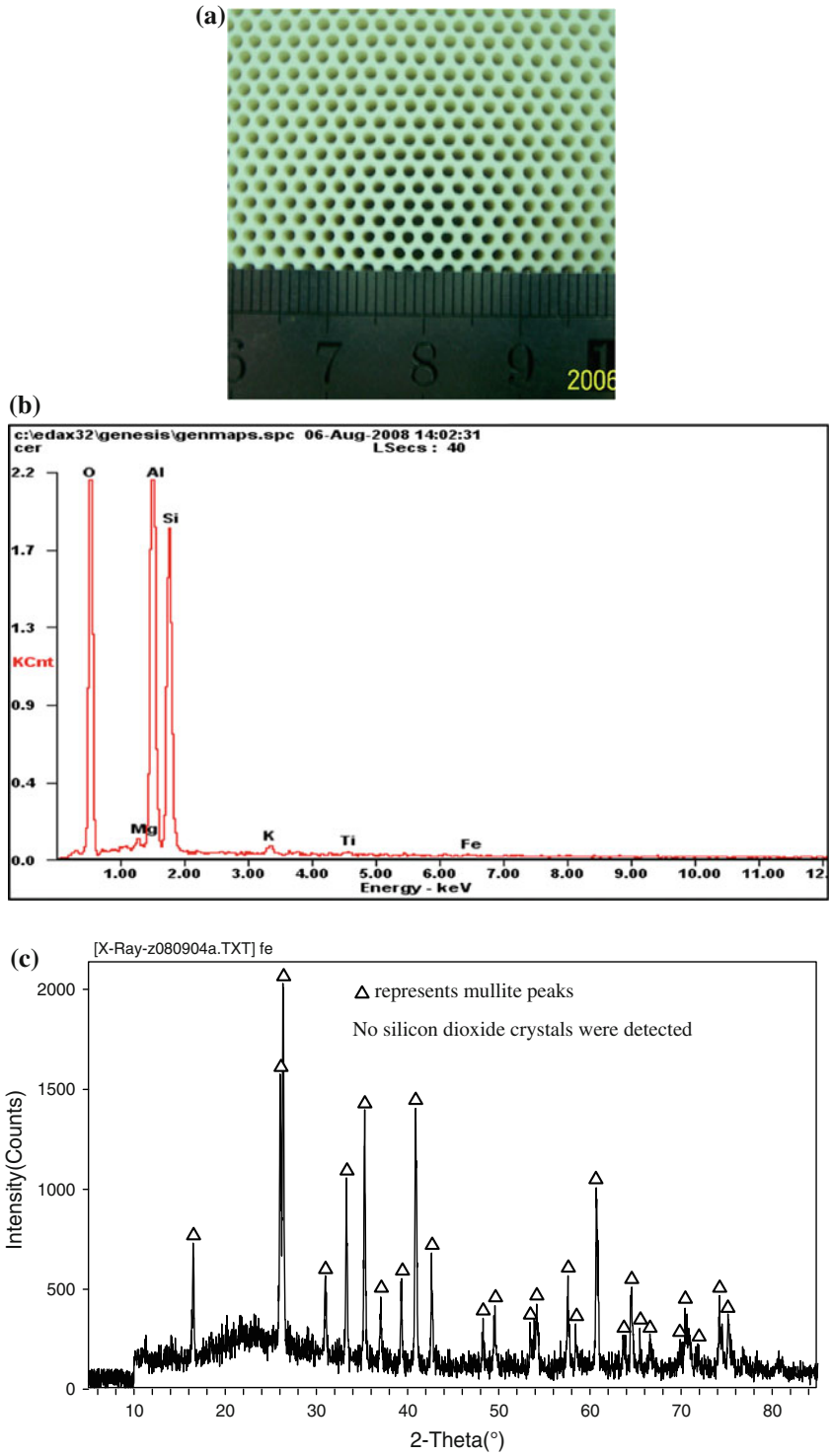

Fig. 1 Ceramic **a** framework diagram, **b** EDS spectrum and **c** powder X-ray diffraction patterns

and hard-alloy specimens, etc. (Fig. 4). It consisted of a quasi-cylinder, a fixing framework and other components. In this experiment, the semi-interpenetrating network composites were employed as an upper specimen and the brake materials as a lower specimen. During installation, the upper specimen was placed into the quasi-cylinder holder and then fixed in a clamp. The lower specimen into the framework and then fastened firmly by two screws to the framework. The upper and lower specimens need to be renewed when worn off with thickness below 6.9 mm. Test stroke and frequency were, respectively, selected as 1 mm and 80 Hz in all cases. The loads of 40, 80, 120 and 160 N,

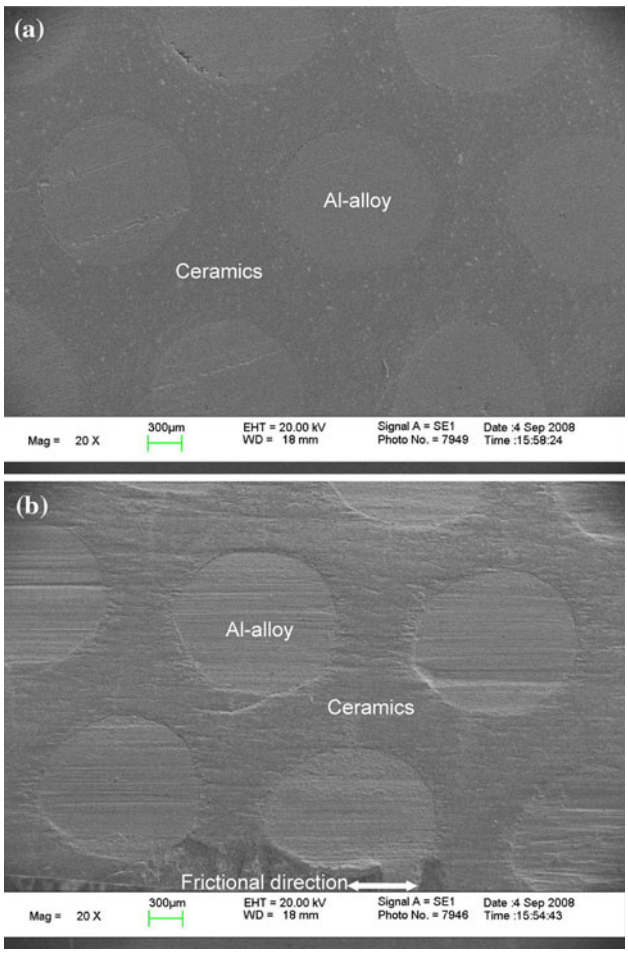

Fig. 2 Semi-interpenetrating network ceramics/Al-alloy composites **a** before testing **b** after testing

equivalent to 1, 2, 3 and 4 MPa, respectively, were applied by a servo system exerted on the quasi-cylinder holder. These values are comparable to routine automobile brake pressures. All the testing procedures were operated by a data acquisition system of a computer.

2.3 Test Method

Based on the preliminary test observations, a test schedule was developed to determine friction levels and wear. It consists of friction fade and recovery, load sensitivities at 100 and 250 °C, as well as temperature and load dependence of wear. Test procedures began with a running-in of at least 20-min duration at a load of 30 N and temperature lower than 90 °C on the SRV testing machine until the apparent contact area between the pad and the composites surpassed 95%. This was followed by a fade run at a load of 40 N where the test temperatures were allowed to rise from 100 to 300 °C. Each temperature test lasted 10 min. At 50 °C intervals, the average friction reading was taken as representative for posterior 5-min duration. During the recovery part of the test the pad was allowed to cool, where the load was applied and friction readings were taken similar to the fade test. The relevant properties of the pad under investigation are given in Fig. 5.

Subsequently, the load sensitivity tests were conducted, where the pad was applied for 10 min at a preset load and temperature. The average friction reading was taken. The tested initial load of 40 N was increased to 160 N in steps of 40 N at 100 and 250 °C, respectively. Each load test began with new pad materials and all the materials were also submitted to the same running-in as above. The relevant properties of the pad are displayed in Fig. 6.

Finally, the wear tests were carried out. Tested temperatures were altered from 100 to 300 °C and loads from 40 to 160 N at 100 and 250 °C, respectively. Each wear test was started with new pad materials and lasted 1 h after the initial running-in so that there was sufficient weight loss generation for comparison. Each test pad was weighed before and after testing, and then each weight loss was expressed as the specific wear rate according to the calculation of the following formula

$$k = \frac{\Delta m}{tlfPd} \tag{1}$$

where k is the specific wear rate of the pad ($mm^3\ N^{-1}\ m^{-1}$), Δm is the pad weight loss (kg), d is the pad density ($kg\ m^{-3}$), P is the applied load (N), l is the oscillation stroke (mm), f is the oscillation frequency (Hz) and t is the total test time (s). The test results under study are shown in Figs. 7 and 8, respectively.

3 Results and Discussion

3.1 Friction Model

The quasi-circular Al-alloy and the surrounding ceramics at the horizontal surface for the composites before tests exhibit light and deep grey colors, respectively (Fig. 2a). The two different colors resulted from some mixing materials that smeared two materials' surfaces. During the initial friction stages, both should rub with the countersurface together, generating a resultant friction coefficient. Nevertheless, the abrasive modes were absolutely distinct when they came in direct contact with hard particles or fibers. The former was more easily worn away to form lowlands, while the latter edges were more rapidly abraded than their centers due to the absence of Al-alloy supporting. This abrasive action eventually made the ceramic centers slightly protrude from the surface. The corresponding SEM photograph for the composites after tests demonstrates that the aforementioned analysis is true (Fig. 2b). A protrusion of the ceramics bore

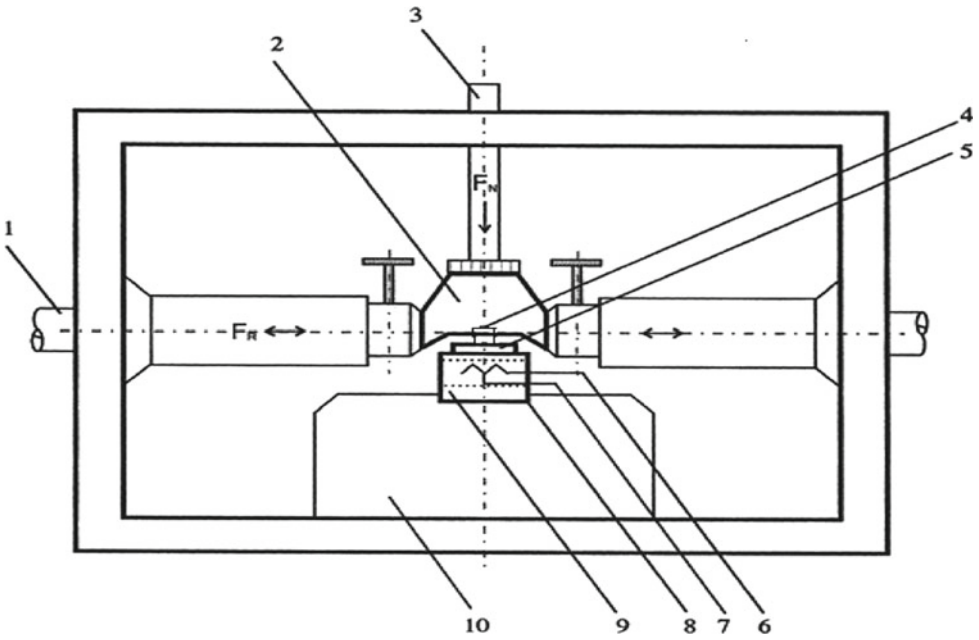

Fig. 3 Schematic view of the SRV test chamber. (*1*) oscillation drive rod, (*2*) upper specimen holder, (*3*) loading device, (*4*) upper specimen, (*5*) lower specimen, (*6*) electrical resistance heating, (*7*) resistance sensor, (*8*) lower specimen holder, (*9*) quartz force transducer, (*10*) supporting block

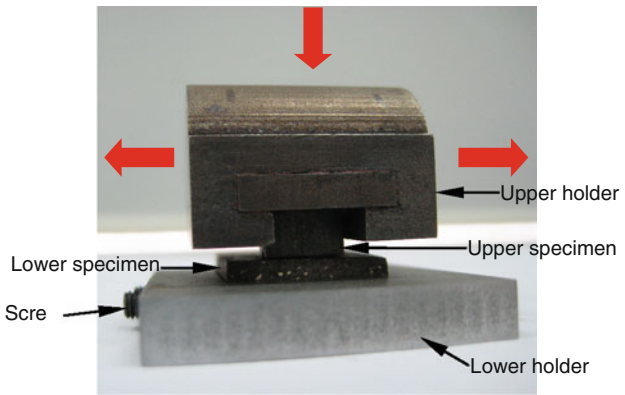

Fig. 4 The original image of the designed holder

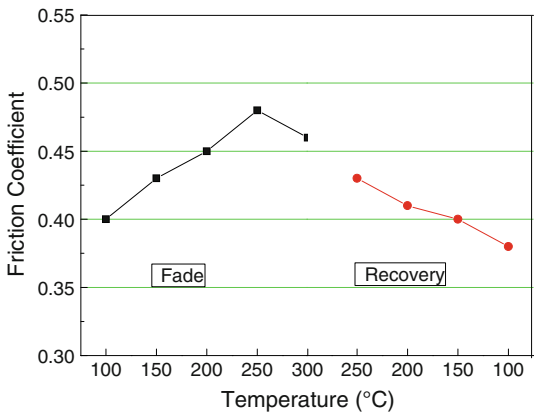

Fig. 5 Friction fade and recovery at $P = 40$ N, $l = 1$ mm and $f = 80$ Hz

main loads, protecting nascent Al-alloy from abrasion in situ, especially, serving as abrader for the pad material due to their high hardness. The speed of the Al-alloy abrasion was reduced consumedly, thereby suggesting that the upper specimen abrasion is expected to be trivial.

The lowlands started to collect various entering wear debris as the friction proceeded, which was forced to accumulate into tribofilms and even further to develop a transfer layer that covered a whole friction surface. Some tribofilms were accumulated and the other expulsed until they were in equilibrium with respect to the accumulation and expulsion between the two partners. The original equilibrium was broken and then new equilibrium was established once the friction conditions (temperature, load, stroke and/or frequency) were altered. Similarly, the so-called lowlands occurred on the pad surface [8]. E-glass fibers were considered a chief supporting ingredient to suppress the abrasion with their highest hardness and percentage in the pad material. Numerous grooves were found at the composites surfaces along the frictional direction (Fig. 2b). The groove width is approximately 0.01 mm, being close to E-glass fiber diameter. The groove length is approximately 1 mm, being equal to the test stroke. This denotes E-glass fibers abraded the composites to form the long, shallow grooves, which features two-body abrasions.

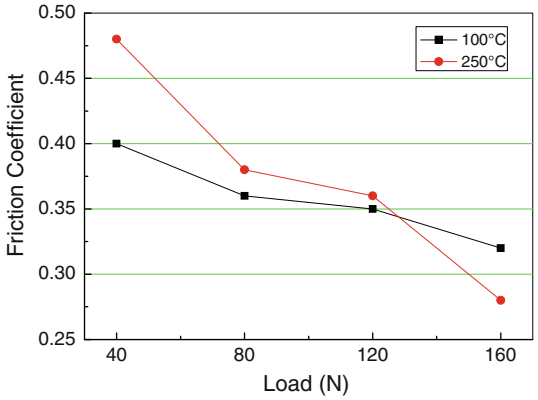

Fig. 6 Load sensitivity: effect of load on the friction coefficient at $l = 1$ mm, $f = 80$ Hz and $T = 100$ and 250 °C

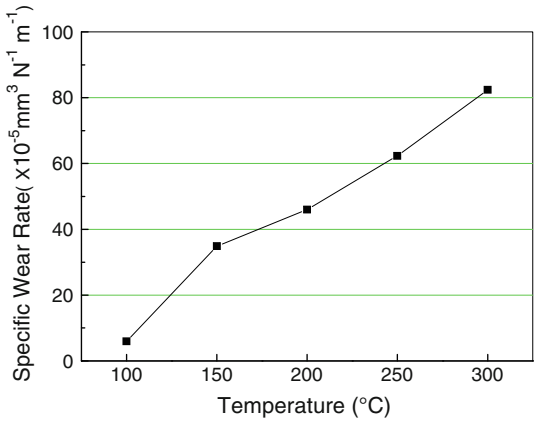

Fig. 7 Effect of temperature on the specific wear rate of brake material at $P = 40$ N, $l = 1$ mm and $f = 80$ Hz

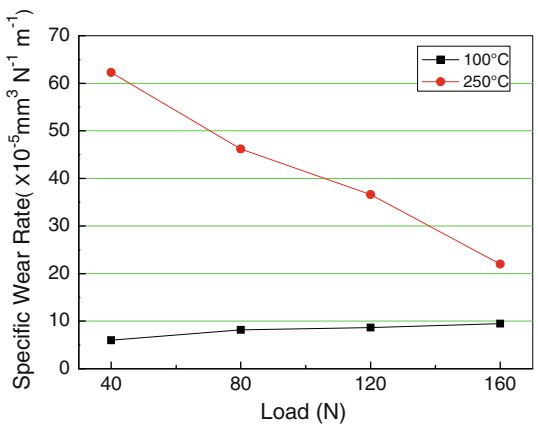

Fig. 8 Effect of load on the specific wear rate of brake material at $l = 1$ mm, $f = 80$ Hz and $T = 100$ and 250 °C

A few wider and deeper grooves may be produced by intermittent rubbing of E-glass fibers many times. A series of parallel ridges appeared adjacent to the grooves whereas abrasive indentations existed chiefly at the ceramic edges. The simplified friction models are illustrated (Fig. 9), as described above.

3.2 Effect of Temperature on Friction and Wear

The friction fade and recovery tests were carried out. During the fade part of the test the friction coefficient first increased and then fell (Fig. 5). It is well known that temperature rise universally accelerates the thermal decomposition of such organic compounds as phenolic resin and wood fiber. The shear strength between the sliding contact surfaces is reduced and so is the friction level. Unfortunately, the experimental results are inconsistent with the known fact at the lower temperatures, meaning that the thermal decomposition plays a less significant role in the friction.

At the end of the wear tests, the worn pad surfaces were used for the analyses of SEM and EDS with the aim of eventually accounting for the inconsistency. The SEM photographs through selection were listed in Fig. 10. Notice that the worn surfaces are relatively rough with recesses, grooves, free-rolling abrasive particles and pulled out E-glass fibers, indicating that different regions for the surfaces were worn down asynchronously. Two bigger recesses exist in Fig. 10a. It is possible that the generating wear debris was small in amount and insufficient to fill the recesses. However, in the localized regimes the compaction of wear debris was evolved into the contact plateaus rising above the rest of the surface. E-glass fibers are invisible in the plateau regimes but visible in the recess regimes, confirming that the plateau surfaces are constituted by tiny wear debris. Also, the analogous plateaus can be perceived in Fig. 10b and c. Their total area recognized with the naked eye increases in conformity with the sequence of a–c. As in all sliding contact situation, adhesive interaction gained in importance during the mixed friction. A high temperature of 300 °C created more tribofilms (abrasions) seen in a subsequent section. They were uneasy to be compressed at the low load owing to the effect of heat stress, and therefore the transfer layer formed in Fig. 10e features incompact wear debris. A series of fine parallel grooves along the frictional direction is visible over a wide range of the surface. Their widths are close to the ridge ones for the Al-alloy surfaces in Fig. 2b. The ridges may be impressed into the transfer layer and then slid with the assistance of tangential shear forces, forming the well-defined grooves. Figure 10d exhibits transition surface traits that the tribofilms are relatively incompact. The friction variation can be explained in light of these observations. More tribofilms generated were entrapped between two partners at elevated temperatures. A part of tribofilms caused the real contact area to augment after filling in some

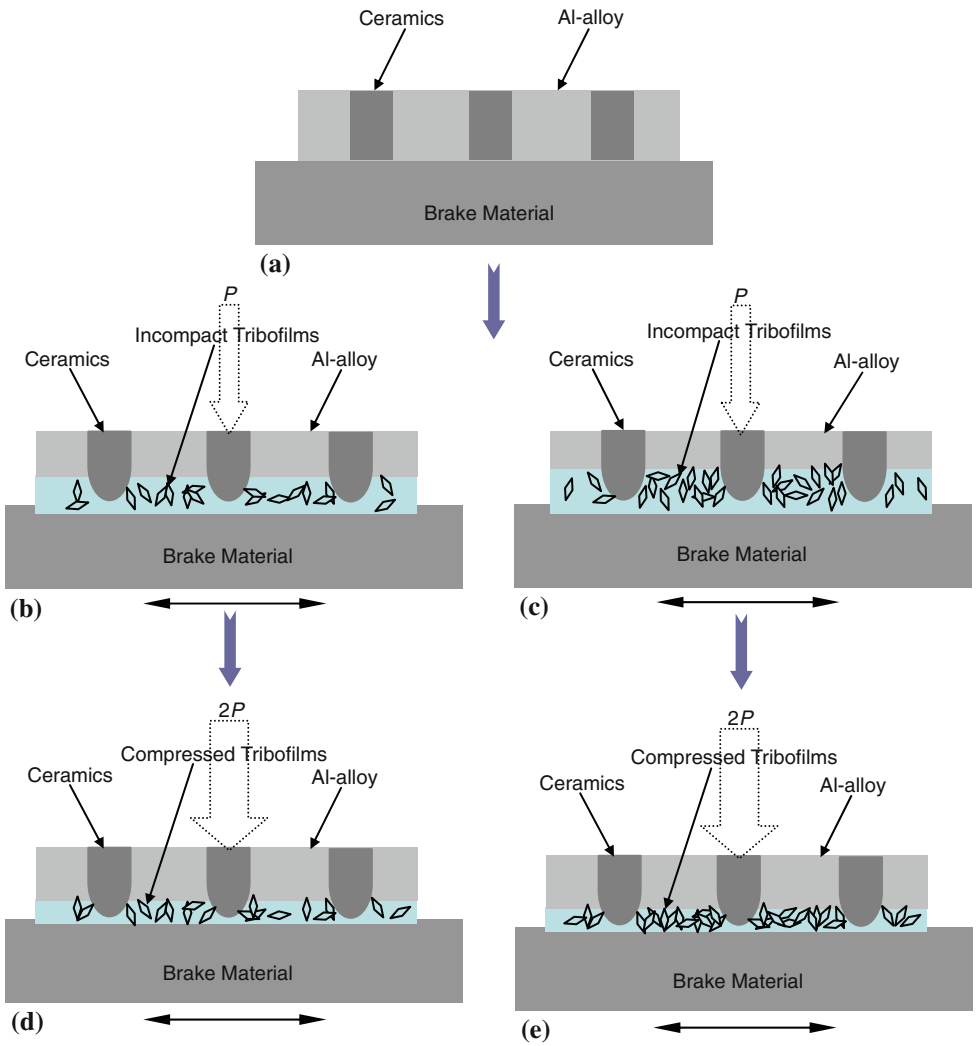

Fig. 9 Brake material versus ceramics/Al-alloy composites in friction models: **a** prior to friction tests, **b** fewer incompact tribofilms, **c** more incompact tribofilms, **d** fewer compressed tribofilms and **e** more compressed tribofilms. Load increases in conformity with the sequence of **b–d** or **c–e**. *Double headed arrows* represent the sliding friction direction

recesses and grooves, but on the other hand, the transfer layer to thicken. The former leads to an increase in the friction coefficient, but the latter to a decrease in the shear strength and sequent friction coefficient. This dual function of the tribofilms contributes to the highest friction level encountered at 250 °C.

During the recovery part of the test, more tribofilms were accumulated at the surface after the pad was submitted to a longer period of rubbing, especially at a high temperature of 300 °C. The frictional equilibrium was broken as temperature fell. The expulsion of the tribofilms was quickened that more E-glass fibers may be exposed at the surfaces. Their glossy surfaces reduced adhesive interactions with the high-content ceramics. The friction level remarkably decreased and even was inferior to that corresponding to the fade part, as given in Fig. 5. This phenomenon displayed in tribology is defined as the inverse recovery. Serious inverse recovery is impermissible pertaining to automotive brake materials. EDS analysis results revealed that the identical ingredient exhibited very similar content at different temperatures and are not reported here.

The wear tests were conduced. The specific wear rate showed an incremental tendency with temperature (Fig. 7). This is relevant with the aggravating decomposition of the organic compounds at elevated temperatures.

3.3 Effect of Load on Friction and Wear

The load sensitivity tests were performed. The friction coefficient is a decreasing function of load at 100 and 250 °C, respectively (Fig. 6). The worn pad surfaces were examined and photographed using SEM after the wear tests. The photographs at 100 °C show that damage to the surfaces grows severer in conformity with the sequence of Fig. 11a–d. The logical explanation of the behaviour is that the pad abrasion is very likely to start with the resin-bonded materials surrounding E-glass fibers and copper fibers

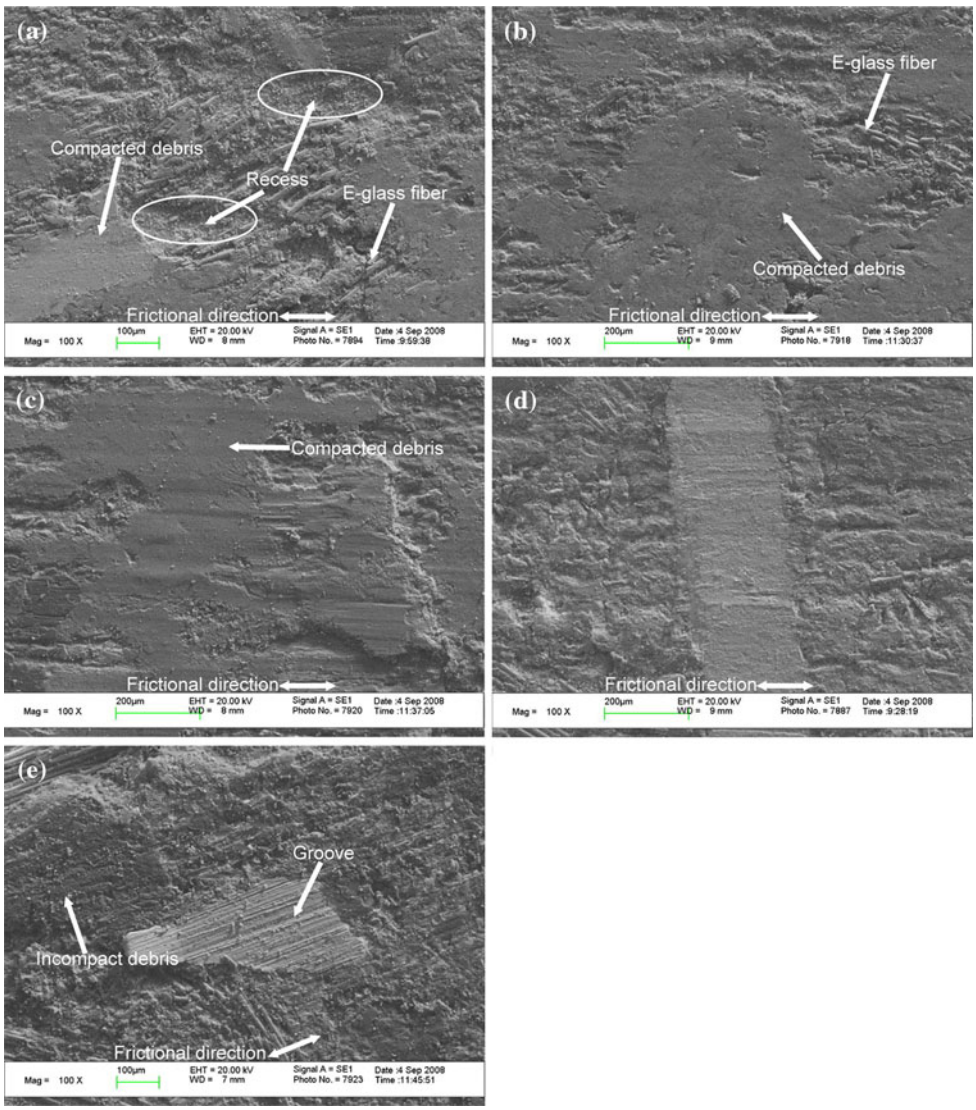

Fig. 10 SEM photographs of brake material subjected to wear test at $P = 40$ N, $l = 1$ mm, $f = 80$ Hz and $T =$ **a** 100 °C, **b** 150 °C, **c** 200 °C, **d** 250 °C and **e** 300 °C

irrespective of few wood fibers, which consisted of some small-size particles (coke/graphite/chromite/barite/red iron oxide). Coke may be crushed into smaller fragments and graphite torn to pieces, whereas the latter three pulled away intact rather than fracture due to their superior fracture toughness. The higher the applied load the deeper the ceramic penetration into the pad. A great penetration depth may result in more subsurface deformation, and thus, more small-particle detachment (abrasions). Thus the formation of wear debris stemmed from a failure to bond with the matrix. At a low load of 40 N, only a small number of resin-bonded materials were removed, so few E-glass fibers can be appreciated in Fig. 11a. Notice in Fig. 11b that E-glass fibers are randomly scattered in different directions and their ends are still embedded into the matrix. This is almost the distribution mode of the original E-glass fibers, confirming that long E-glass fibers were not easily pulled out of the matrix. At higher load of 120 or 160 N, a relatively large material removal by deformation promoted E-glass fiber pullout or fracture from the matrix. Some E-glass fibers failed to be broken into tiny fragments. Those left behind at the worn surface were compelled to lie low (Fig. 11c and d). Their glossy surfaces rubbed with the ceramics, lowering the friction, as mentioned in a previous section.

The SEM photographs at 250 °C are given in Fig. 12. A comparison with the surface topographies in Figs. 11 and 12 shows the coverage of the tribofilms at 100 °C is less intense than that at 250 °C with respect to identical loads, which has direct relation with the difference in the pad abrasion seen in a later section. The presence of numerous E-glass fibers suggests the tribofilms generated have largely escaped from the worn surface (Fig. 12a). Figure 12b shows relatively smooth and featureless surface except for

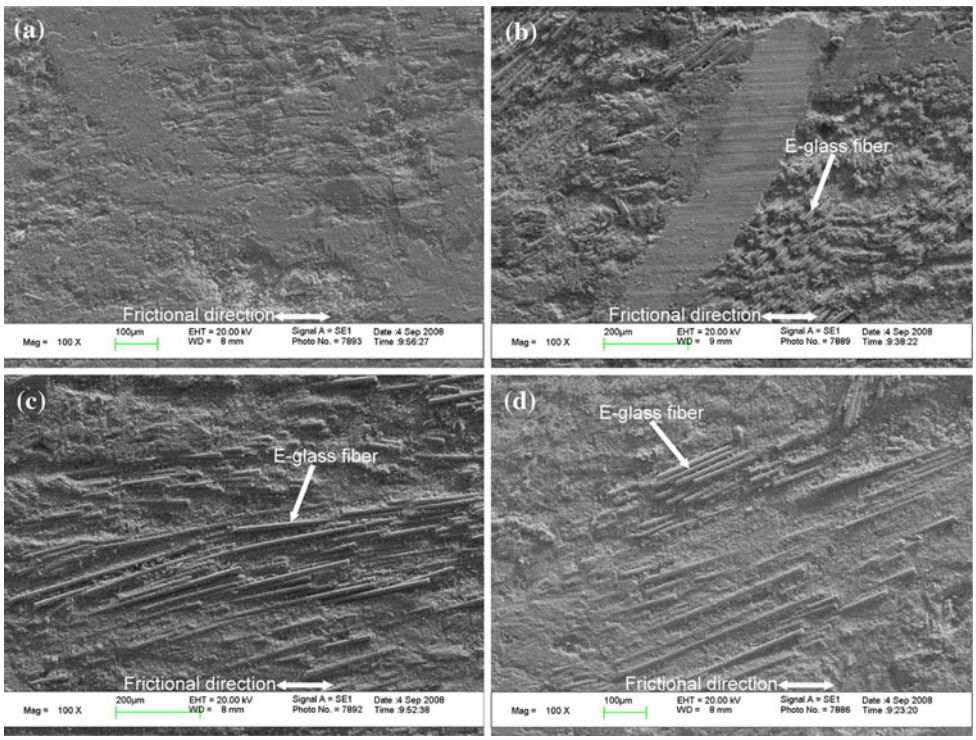

Fig. 11 SEM photographs of brake material subjected to wear test at $T = 100$ °C, $l = 1$ mm, $f = 80$ Hz and $P =$ **a** 40 N, **b** 80 N, **c** 120 N and **d** 160 N

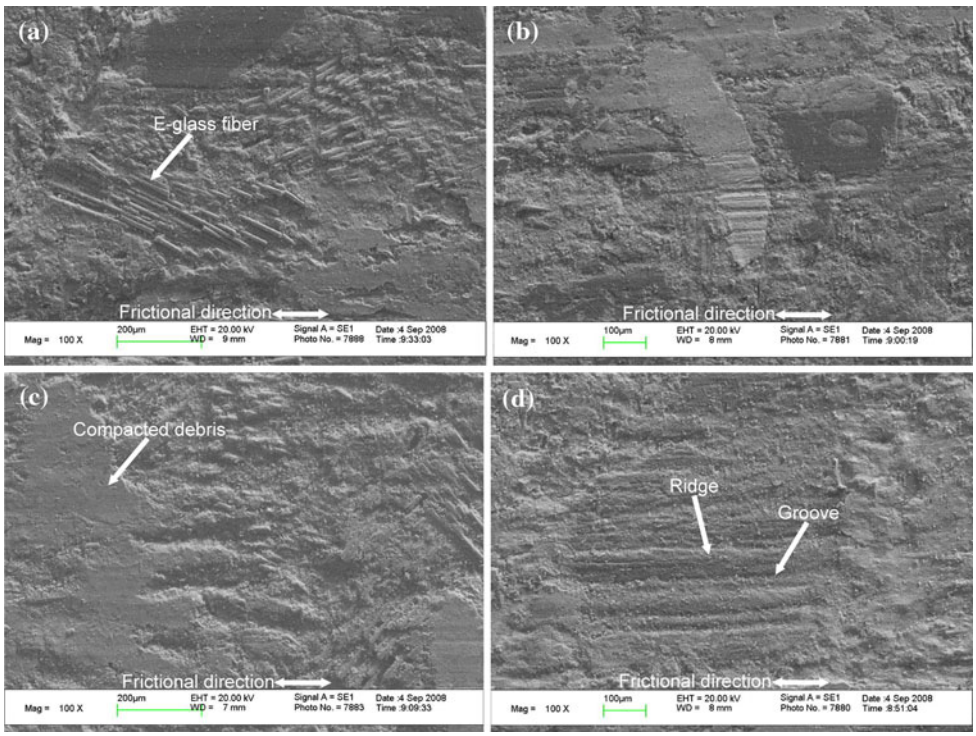

Fig. 12 SEM photographs of brake material subjected to wear test at $T = 250$ °C, $l = 1$ mm, $f = 80$ Hz and $P =$ **a** 40 N, **b** 80 N, **c** 120 N and **d** 160 N

light rubbing tracks. Features of typical compacted debris and severe matrix damage are observed in Fig. 12c. However, the worn surface is obviously filled with the tribofilms (Fig. 12d), where several short and parallel grooves are present. The ceramic asperities at the edges may be penetrated into the pad material and then ploughed across the surface to form the short grooves. A large amount of wear debris was eventually piled up and compacted into the ridges along the sides of the grooves, indicating that the removal of the tribofilms from the worn

surfaces is a formidable task once they are compressed at higher loads. This unsuccessful removal is responsible for a reduction in the friction.

The chemical ingredients and contents at different regions of the worn pad surfaces were determined using EDS to further investigate the influence of tribofilms on the friction and wear. The relevant average data of eight test results under the same conditions are given in Table 1. If some trace elements were neglected, Al and Mg were merely derived from the composites; C, Cu, S, Ba, Ca and Fe principally from the brake materials; Si, Zn and Cr from the two materials together. In the case of atomic percentage, C, Si, Fe, Al and Cu were taken into account as crucial elements in the following investigations, since they almost ranked in the top five among all the detected elements regardless of O. Simple substances such as Fe, Al and Cu are oxidized rapidly into their respective oxides, especially at their surface layers but have inability to be converted into other compounds in great numbers owing to the impermanency of the actual friction process. Based on these considerations, the possible existence forms of Cu, Fe, Al, and Si after tribochemical reactions contain Cu_2O, CuO, Fe_2O_3, Fe_3O_4, FeO, Al_2O_3, SiO_2, $Cr_2O_3{\cdot}Fe_2O_3$, $5Al_2O_3{\cdot}8SiO_2$, $3Al_2O_3{\cdot}2SiO_2$, $Na_2SiO_3{\cdot}CaSiO_3$, etc. Normally, the former five are considered as mild abrasives; the latter six as severe abrasives whereas coke and graphite, two existence forms of C, as solid lubricants as per their hardness magnitude [9]. Figure 13 plots the atomic percentages of the investigated five elements as a function of load at 100 and 250 °C, respectively, where comparison with the data at 100 and 250 °C shows that little has changed about Fe content over the wide load range. Cu has relatively low content in both cases and, in particular, the corresponding oxides belong to mild abrasives. Therefore, the influence of Fe and Cu on the friction and wear are deemed to be nonsignificant. It can also be noted that Si and Al contents at 100 °C are basically greater than those at 250 °C, but C content exhibits an opposite tendency. One of the reasons for the existence of high-content C at 250 °C is that the conversion of coke and graphite into CO and CO_2 through tribochemical reactions was incomplete due to very quick abrasion. Large amounts of unreacted coke and graphite were retained in the tribofilms. These tribofilms should possess a better compressibility than the ones at 100 °C since coke is a typical kind of porous material. The lower Al content detected implies that the tribofilms formed this way were predominantly produced from the pad rather than the composites. This coincides with the expected result in the friction models. The weight loss for the composites was therefore negligible and is not reported here.

Table 1 EDS analysis conducted on the worn brake material surface at different temperatures and loads

Element	Atomic percentage							
	100 °C				250 °C			
	40 N	80 N	120 N	160 N	40 N	80 N	120 N	160 N
C	20.20	11.91	8.52	10.75	21.53	25.71	15.10	22.84
O	42.64	46.58	46.36	42.44	39.04	42.70	47.50	40.62
Mg	1.60	2.04	1.87	1.66	1.48	1.32	1.80	1.72
Al	5.95	6.40	5.86	6.96	5.79	4.76	4.94	4.62
Si	11.64	14.69	13.50	12.32	9.18	9.58	13.58	10.87
S	1.05	0.46	1.47	0.80	1.14	1.22	1.16	0.92
Ca	3.23	4.42	4.36	3.54	2.48	2.68	4.14	3.04
Cr	0.45	0.34	0.48	0.36	0.38	0.44	0.52	0.35
Fe	9.58	5.30	7.39	6.82	6.44	6.06	7.18	5.5
Ba	2.02	1.50	2.29	2.01	1.98	1.76	2.15	1.68
Zn	1.25	1.98	2.82	4.22	3.71	1.28	0.54	2.56
Cu	2.38	4.38	5.07	8.12	6.85	2.50	1.38	5.28

A close look at both curves in Fig. 6 shows that the friction coefficients converged gradually to an intersecting point and then diverged at 100 and 250 °C, where the load value is approximately 128 N (3.2 MPa). Returning to the friction models (Fig. 9) to facilitate understanding of the tribological phenomena, in the case of two rubbing partners, as load increases, so does the total area of micro-contacts [10]. This area increase chiefly makes partial loads shifted from the ceramics to the tribofilms. In short, the tribofilms bear the increasing relative loads. This gives rise to a reduction in the friction. At 100 °C, there existed fewer tribofilms and, with them, less graphite and coke with friction-reducing action as well as more compounds (corresponding to Si and Al) with friction-increasing action as compared with those at 250 °C. Hence, the friction coefficient was less sensitive to applied load. On the contrary, at 250 °C there existed more tribofilms. This included more graphite and coke as well as fewer compounds (corresponding to Si and Al). In the low-load regime lower than 128 N, despite more tribofilms generation, these incompact tribofilms were expulsed rapidly. Their filling action of some recesses and grooves is identified as the primary contribution to the friction, the friction being higher than that at 100 °C while in the high-load regime more than 128 N the friction exhibited an inverse tendency. Some of the reasons are that the tribofilms obtained a stronger compression, the friction-reducing action of graphite and coke became relatively stronger but the friction-increasing action of the compounds (corresponding to Si and Al) became relatively weaker.

The final wear tests were conducted. The specific wear rate as a function of load at 100 and 250 °C is shown in Fig. 8. The latter specific wear rate exceeded the former, as expected. Notice that the former specific wear rate merely mildly increased throughout the test. Normally, fewer

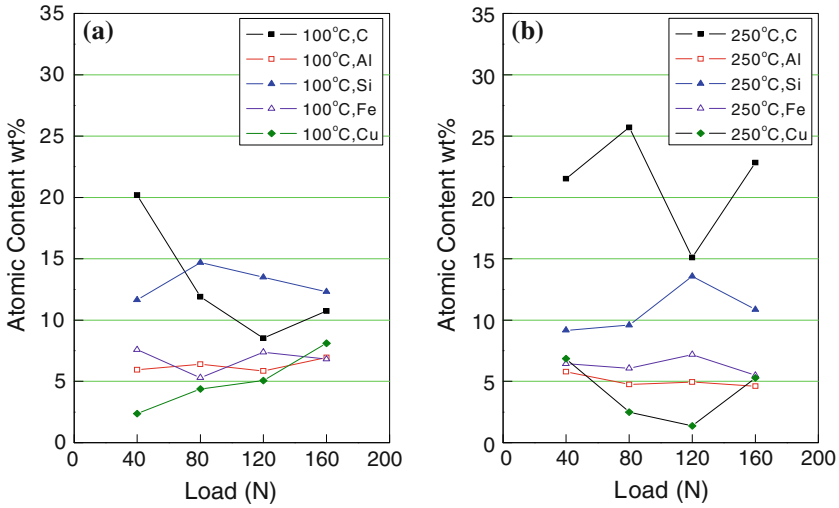

Fig. 13 Comparison of the influences of load on the main atomic percentages on the worn brake material surface at $T =$ **a** 100 °C and **b** 250 °C

tribofilms at 100 °C were insufficient to protect the pad from abrasion. Moreover, less graphite and coke reduced antiwear action, and more compounds (corresponding to Si and Al) enhanced three-body abrasive action when serving as free-rolling abrasive particles. Following these analyses, we are able to draw an improper conclusion that the pad wear resistance markedly decreases. Accordingly, the mild increase in the specific wear rate should be attributed to the existence of numerous E-glass fibers shown in Fig. 11b–d. They suppressed larger abrasions, as predicted in the friction models. It can still be noted that the latter specific wear rate dropped dramatically with the increase of load. This situation is explicitly connected with the friction variation (Fig. 6). The thickening of the transfer layer (or the augmentation of the tribofilms) effectively shielded the pad from the sharp cutting asperities. Further contributions of the tribofilms still include the promotion of antiwear action induced by more graphite and coke and the mitigation of the three-body abrasion induced by fewer compounds (corresponding to Si and Al).

As far as routine brake systems with gray cast iron rotors are concerned, the maximum allowable value of the specific wear rate is 10^{-4} mm^3 N^{-1} m^{-1} for this type of brake material. The current specific wear rates are found which have partly surpassed the value. This is unacceptable in commercial applications.

4 Conclusions

The friction and wear properties of the brake materials dry sliding against the semi-interpenetrating network ceramics/Al-alloy composites strongly depend on temperature, load and, with them, tribofilms.

For a temperature range from 100 to 250 °C, the friction rise is attributed to the increase of the real contact area between the sliding countersurfaces relevant to some recesses and grooves filled with the tribofilms, but with temperature going up to 300 °C the aggravating decomposition of the organic compounds leads to the friction fade. The inverse recovery took place upon cooling. Wear showed an incremental tendency with temperature.

The load sensitivity tests were performed. The friction was found to decrease with the increase of load at 100 and 250 °C. At load levels of 40–128 N, the former friction was inferior to the latter, since the filling action of the tribofilms is identified as the primary contribution to the friction. At load levels of 128–160 N, the tribofilms at 250 °C were strongly compressed, inclusive of more graphite and coke as well as fewer compounds (corresponding to Si and Al) compared with those at 100 °C, inducing a large decrease in the friction. At 100 °C the glossy surfaces of E-glass fibers exposed at the worn surfaces decreased the friction, but fewer tribofilms and, with them, less graphite and coke as well as more compounds (corresponding to Si and Al) impeded the decrease. The friction becomes less sensitive to applied load. The wear tests were also carried out. Wear at 100 °C mildly increased with load due to the suppression action of E-glass fibers, while at 250 °C, it dropped dramatically associated with the protection of more tribofilms including more graphite and coke, and fewer compounds (corresponding to Si and Al). The proposed friction models incorporated with SEM and EDS analyses explain the experimental results better.

Acknowledgement The authors wish to thank WKT brake Co. Ltd for its technical help.

References

1. Shorowordi, K.M., Haseeb, A.S.M.A., Celis, J.P.: Velocity effects on the wear, friction and tribochemistry of aluminum MMC sliding against phenolic brake pad. Wear **256**, 1176 (2004)

2. García-Cordovilla, C., Narciso, J., Louis, E.: Abrasive wear resistance of aluminium alloy/ceramic particulate composites. Wear **192**, 170 (1996)
3. Prasad, S.V., Asthana, R.: Aluminum metal-matrix composites for automotive applications: tribological considerations. Tribol. Lett. **17**, 448 (2004)
4. Gopal, P., Dharani, L.R., Blum, F.D.: Load, speed and temperature sensitivities of a carbon-fiber-reinforced phenolic friction material. Wear **181–183**, 913 (1995)
5. Zhang, S.Y., Wang, F.P.: Comparison of friction and wear performances of brake material dry sliding against two aluminum matrix composites reinforced with different SiC particles. J. Mater. Process. Technol. **182**, 125 (2007)
6. Jang, H., Ko, K., Kim, S.J., Basch, R.H., Fash, J.W.: The effect of metal fibers on the friction performance of automotive brake friction materials. Wear **256**, 412 (2004)
7. Zhang, S.Y., Wang, F.P.: Comparison of friction and wear performances of brake materials containing different amounts of $ZrSiO_4$ dry sliding against SiC_P reinforced Al matrix composites. Mater. Sci. Eng. A **443**, 243 (2007)
8. Eriksson, M., Jacobson, S.: Tribological surfaces of organic brake pads. Tribol. Int. **33**, 821 (2000)
9. Nicholson, G.: One Hundred Years of Friction Material. P&W Price Enterprises, Inc., Winchester (1995)
10. Straffelini, G.: A simplified approach to the adhesive theory of friction. Wear **249**, 81 (2001)